



This discussion paper is/has been under review for the journal Atmospheric Chemistry and Physics (ACP). Please refer to the corresponding final paper in ACP if available.

# Atmospheric boundary layer top height in South Africa: measurements with lidar and radiosonde compared to three atmospheric models

K. Korhonen<sup>1,2</sup>, E. Giannakaki<sup>1</sup>, T. Mielonen<sup>1</sup>, A. Pfüller<sup>1</sup>, L. Laakso<sup>3,4</sup>, V. Vakkari<sup>3,5</sup>, H. Baars<sup>6</sup>, R. Engelmann<sup>6</sup>, J. P. Beukes<sup>4</sup>, P. G. Van Zyl<sup>4</sup>, A. Ramandh<sup>7</sup>, L. Ntsangwane<sup>8</sup>, M. Josipovic<sup>4</sup>, P. Tiitta<sup>2,9</sup>, G. Fourie<sup>7</sup>, I. Ngwana<sup>8</sup>, K. Chiloane<sup>10</sup>, and M. Komppula<sup>1</sup>

<sup>1</sup>Finnish Meteorological Institute, P.O. Box 1627, 70211, Kuopio, Finland

<sup>2</sup>Department of Applied Physics, University of Eastern Finland, P.O. Box 1627, 70211 Kuopio, Finland

<sup>3</sup>Finnish Meteorological Institute, P.O. Box 503, 00101, Helsinki, Finland

<sup>4</sup>School of Physical and Chemical Sciences, North-West University, Potchefstroom, South Africa

<sup>5</sup>Department of Physics, University of Helsinki, P.O. Box 64, 00014 Helsinki, Finland

<sup>6</sup>Leibniz Institute for Tropospheric Research, Permoserstrasse 15, 04318, Leipzig, Germany

<sup>7</sup>Sasol Technology R&D (Pty) Ltd., P.O. Box 1, Sasolburg, South Africa

<sup>8</sup>South African Weather Service, Pretoria, South Africa

Title Page

Abstract

Introduction

Conclusions

References

Tables

Figures



Back

Close

Full Screen / Esc

Printer-friendly Version

Interactive Discussion



<sup>9</sup>Department of Environmental Sciences, University of Eastern Finland, P.O. Box 1627, 70211 Kuopio, Finland

<sup>10</sup>Eskom Holdings SOC Ltd; Sustainability Division; Research, Testing and Development, South Africa

Received: 16 April 2013 – Accepted: 11 June 2013 – Published: 1 July 2013

Correspondence to: M. Komppula (mika.komppula@fmi.fi)

Published by Copernicus Publications on behalf of the European Geosciences Union.

## ACPD

13, 17407–17450, 2013

### Atmospheric boundary layer top height in South Africa

K. Korhonen et al.

Title Page

Abstract

Introduction

Conclusions

References

Tables

Figures



Back

Close

Full Screen / Esc

Printer-friendly Version

Interactive Discussion



## Abstract

Atmospheric lidar measurements were carried out at Elandsfontein measurement station, on the eastern Highveld approximately 150 km east of Johannesburg in South Africa (SA) throughout 2010. The height of the planetary boundary layer (PBL) top was continuously measured using a Raman lidar, Polly<sup>XT</sup> (**POrtabLe Lidar sYstem eXTended**). High atmospheric variability together with a large surface temperature range and significant seasonal changes in precipitation were observed, which had an impact on the vertical mixing of particulate matter (PM), and hence, on the PBL evolution. The results were compared to radio soundings, CALIOP (Cloud–Aerosol Lidar with Orthogonal Polarization) space-borne lidar measurements and three atmospheric models that followed different approaches to determine the PBL top height. These models included two weather forecast models operated by ECMWF (European Centre for Medium-range Weather Forecasts) and SAWS (South African Weather Service) and one mesoscale prognostic meteorological and air pollution regulatory model TAPM (The Air Pollution Model). The ground-based lidar used in this study was operational for 4935 h during 2010 (49 % of the time). The PBL top height was detected 86 % of the total measurement time (42 % of the total time). Large seasonal and diurnal variations were observed between the different methods utilised. Comparison of lidar measurements to the models indicated that the ECMWF model agreed the best with mean absolute difference of 15.4 %, while the second best correlation was with the SAWS model with corresponding difference of 20.1 %. TAPM was found to have a tendency to underestimate the PBL top height. The wind speeds in SAWS operated and TAPM models were strongly underestimated which probably led to underestimation of the vertical wind and turbulence and thus underestimation of the PBL top height. High variation was found when lidar measurements were compared to radiosonde measurements. This could be partially due to the distance between the lidar measurements and the radiosondes, which were 120 km apart. Comparison between ground-based and satellite lidar shows good agreement with a correlation coefficient of 0.88. On average

## Atmospheric boundary layer top height in South Africa

K. Korhonen et al.

Title Page

Abstract

Introduction

Conclusions

References

Tables

Figures



Back

Close

Full Screen / Esc

Printer-friendly Version

Interactive Discussion







---

## Atmospheric boundary layer top height in South Africa

K. Korhonen et al.

---

Title Page

Abstract

Introduction

Conclusions

References

Tables

Figures



Back

Close

Full Screen / Esc

Printer-friendly Version

Interactive Discussion



crophysical properties. A detailed characterization of aerosol properties, vertical stratification, mixing, and aging behaviour of aerosols in West Africa has been performed based on a unique dataset of spectrally resolved backscatter and extinction coefficients and the depolarization ratio (Ansmann et al., 2009). Authors studied the complex layer structure of Sahara dust and biomass burning aerosols observed at Praia, Cape Verde and how the African plume reached the South American coast. Campbell et al. (2003) have found lidar ratios between 50 and 90 sr with the Ångström exponent of 1.5–2 for dense biomass smoke event during SAFARI 2000. They studied backscatter profiles from a micropulse lidar system and compared the results to Sun photometer aerosol optical depth measurements. However, lidar studies in SA are mostly limited to specific case studies. The new generation of space-borne backscatter lidar systems has given insight on the vertical distribution of aerosols in the atmosphere on almost global scale. For example, Liu et al. (2011) analyzed the first two and a half years of the Cloud–Aerosol Lidar with Orthogonal Polarization (CALIOP) data and found a mean of effective lidar ratio of 38.5 sr at 532 nm and 50.3 sr at 1064 nm over North Africa. Despite the large amount of global dust data derived from CALIOP, there are known limitations associated with the elastic backscatter measurement technique and thus the PBL top retrieval.

In this study we conducted continuous long-term ground-based lidar measurements at Elandsfontein in the SA throughout the year 2010 in the framework of the EUCAARI (European Integrated Project on Aerosol Cloud Climate and Air Quality Interactions) project (Kulmala et al., 2011). This is a relatively polluted region where the number of previous atmospheric measurement campaigns has been limited. In this study we compared one year of PBL top height data retrieved from a ground-based lidar measurements with radio soundings, three atmospheric models and a space-borne lidar retrievals. We applied different methods for PBL top height determination for highly varying meteorological conditions. This study is the first long term study of PBL top heights and PBL growth rates in the Southern Hemisphere. Only a few studies have been performed in Europe and Asia, most of them with less data coverage.

## 2 The measurement site

The lidar measurement site was located on a hill top at Elandsfontein (26°15′ S, 29°26′ E, 1745 m a.s.l., which is situated in the eastern part of the Highveld region (Fig. 1) in SA. The Highveld is a large plateau that covers 400 000 km<sup>2</sup>, with average mean altitude of 1500 m a.s.l., varying from 1400 up to 1800 m a.s.l. (Fig. 1). The local time (LT) zone is UTC + 2 and LT has been used in all data in the following text. The station is located about 150 km east from the Johannesburg–Pretoria megacity, the largest metropolitan area in the SA with a population of over 10 million people (Lourens et al., 2012). The surroundings close to the Elandsfontein site are mostly rural with agriculture activities, while the larger region includes mining and industrial activities. Laakso et al. (2012) gave a detailed description of the measurement site.

The main anthropogenic emission sources in this area include high-capacity power production with coal-fired power plants (Lourens et al., 2011), yielding nearly half of all electricity produced on the African continent. In addition, there are many other industrial sources of nitrogen and sulphuric oxides, such as petrochemical industry and mining activities. The area surrounding the measurement site is globally regarded as one of the top five hotspots of nitrogen oxide emissions (Lourens et al., 2011, 2012). Other anthropogenic emissions in this area include household combustion (for space heating and cooking) and controlled, as well as uncontrolled burning of vegetation. Wildfires and controlled burning of vegetation fields are significant sources of particulate emissions, especially during the dry season (April–September). During the measurement campaign the fire frequency in the surroundings of Elandsfontein was highest during September (the end of the dry season), and the lowest and the lowest in March (the end of the wet season) (<http://earthdata.nasa.gov/data/near-real-time-data/firms>).

Four major synoptic circulation types are responsible for most of the atmospheric transport of aerosols and gaseous pollutants over southern Africa (Schulze, 1965; Preston-Whyte and Tyson, 1988). The frequency of occurrence of each of these circulation patterns varies seasonally. The most frequent synoptic-scale circulation type

### Atmospheric boundary layer top height in South Africa

K. Korhonen et al.

Title Page

Abstract

Introduction

Conclusions

References

Tables

Figures



Back

Close

Full Screen / Esc

Printer-friendly Version

Interactive Discussion



over southern Africa is the continental anticyclonic circulation that occurs up to 70 % of the time during winter and 20 % of the time in summer (Tyson et al., 1996).

A dominant characteristic of the SA Highveld climate is the variation between wet (October–March) and dry seasons (April–September). Approximately 90 % of the annual precipitation falls during the wet season. The limited cloud cover during the dry season results in strong nocturnal inversions and reduced vertical mixing at night-time (Laakso et al., 2012) while during day-time strong surface heating and thus vertical mixing occurs. In contrast, the cloudiness and precipitation increase dramatically during the rainy season. This affects the characteristics of PBL in two ways. First, cloudiness affects the solar radiation reaching the earth's surface and thus weakens convective mixing. Secondly, wet soil (due to intensive rainfall) has greater heat capacity than dry soil, which reduces the adiabatic heating of air by the surface and thus weakens the convective mixing.

Meteorological quantities at Elandsfontein were measured with a Vaisala WXT510 meteorological station. Figure 2a shows the annual cycle of temperature during 2010. The hottest month was February, while July was the coldest month with average temperatures of 18.5 °C and 9.4 °C, respectively. The annual average temperature was 15.4 °C. The temperature cycle in 2010 agreed well with long-term climate statistics. The annual average temperature measured for 2010 was 0.5 °C lower than the annual average temperature observed between 1961 and 1990 (World Meteorological Organization, <http://www.worldweather.org/035/c00139.htm>).

Figure 2b shows the monthly averages of daily maximum global radiation (GR) intensities measured on site using a Kipp & Zonen CMP21 pyranometer. The seasonal cycle shows that the highest daily intensities were measured in February (1114 W m<sup>-2</sup>), which was also the hottest month. Lowest maximum intensities were observed in the coldest months, i.e. June and July, when 706 W m<sup>-2</sup> and 713 W m<sup>-2</sup> were measured respectively.

**Atmospheric  
boundary layer top  
height in South Africa**

K. Korhonen et al.

Title Page

Abstract

Introduction

Conclusions

References

Tables

Figures



Back

Close

Full Screen / Esc

Printer-friendly Version

Interactive Discussion



### 3 Methods

#### 3.1 Polly<sup>XT</sup> lidar instrument

The ground-based lidar used in this study is the seven-channel Raman lidar, Polly<sup>XT</sup> (POrtabLe Lidar sYstem eXTended, Althausen et al., 2009), designed for continuous measurements of vertical profiles of both particle and molecular backscatter and extinction. The instrument is entirely remotely controlled via an internet connection, and measurements, data transfer and built-in device regulation are performed automatically. Weekly maintenance visits to the site were carried out to ensure the quality of the measurements.

The Polly<sup>XT</sup> lidar uses a Continuum Inlite III type laser. The pulse rate of the laser is 20 Hz and it delivers energies of 180 mJ, 110 mJ, and 60 mJ simultaneously at the three different wavelengths, i.e. 1064 nm, 532 nm, and 355 nm, respectively. The vertical resolution of the system is 30 m and the vertical range covers the whole troposphere under cloudless conditions. A detailed description of the Polly<sup>XT</sup> lidar system can be found in Althausen et al. (2009).

During the measurement period, vertical profiles of particle backscatter coefficients at 355, 532 and 1064 nm, extinction coefficient at 355 and 532 nm and the linear particle depolarization ratio at 355 nm were obtained from the instrument. The measurement of the height and diurnal evolution of the PBL top was based on the analysis of aerosol layers, derived from vertical backscattering profiles at the wavelength of 1064 nm. Table 1 presents the relevant properties of Polly<sup>XT</sup> used in this study, together with the properties of the other techniques utilised. The other techniques will be discussed in subsequent paragraphs.

#### 3.2 Radio soundings

The data acquired from radio sounding are typically vertical profiles of temperature, pressure, relative humidity (RH), wind speed, and wind direction. By using the obtained

Title Page

Abstract

Introduction

Conclusions

References

Tables

Figures



Back

Close

Full Screen / Esc

Printer-friendly Version

Interactive Discussion



## Atmospheric boundary layer top height in South Africa

K. Korhonen et al.

Title Page

Abstract

Introduction

Conclusions

References

Tables

Figures

◀

▶

◀

▶

Back

Close

Full Screen / Esc

Printer-friendly Version

Interactive Discussion



meteorological data, the PBL height can be derived. For this study, we used radio soundings which were launched at Pretoria (25°33' S, 28°8' E, 1523 m a.s.l.), 120 km northwest from the lidar site. This site is the closest site where such measurements are conducted on a regular basis. The sounding site is being operated by the South African Weather Service (SAWS) and the sondes are launched twice a day at fixed times, 10:00 and 22:00 LT. Other relevant parameters are presented in Table 1.

### 3.3 The ECMWF model

The European Centre for Medium-range Weather Forecasts (ECMWF) runs a global weather forecast model as part of an integrated forecast system. The model version used in this study became operational on the 26 January 2010. Table 1 presents the model properties relevant for this study (ECMWF, 2010a). The total time of each model run is 240 h, while the temporal resolution is three hours for the first 72 h and six hours after this initial period. For this study we chose the four closest grid points surrounding the Elandsfontein lidar site, at distances of 24.5, 16.8, 18.8 and 5.9 km. The PBL height for the lidar site was interpolated using distance-weighted averages of these four data points. The relevant properties of the ECMWF model are summarised in Table 1.

### 3.4 The SAWS operated model

The SAWS operates a regional Unified Model (UM) for local weather forecasts. It is run at 12 km horizontal resolution with 38 vertical levels to produce 48 h forecast, with and without data assimilation. Temporal resolution of the output ranges from minutes to hours. However, in this study we used the archived SA domain data which has 16 vertical levels at our site with a 1 h resolution (Table 1). Due to the comparison to the ECMWF model we chose to use a temporal resolution of three hours for the SAWS model. The 16 model levels cover pressure levels from 850 hPa to 100 hPa with an interval of 50 hPa. Under typical South African climatic conditions the vertical grid extends from the ground level up to approximately 16 km above ground level (AGL).



backscatter (parallel plus perpendicular) at 532 and 1064 nm, as well as the 532 nm perpendicular backscatter. There are three basic types of level 2 data products: layer products, profile products and the vertical feature mask (VFM). Layer products provide layer-integrated or layer-averaged properties of detected aerosol and cloud layers. Profile products provide retrieved extinction and backscatter profiles within these layers. Operational CALIOP PBL product is currently not available. The relevant properties of CALIOP are summarised in Table 1.

### 3.7 Determination of PBL top height and growth rate

#### 3.7.1 Ground-based Lidar: Wavelet Covariance Transform

The PBL top heights were retrieved from the lidar backscatter signal at 1064 nm using the Wavelet Covariance Transform (WCT) method (Brooks, 2003). We chose this method because it allows larger adjustability and thus more robust analysis of the PBL height than e.g. the gradient method. The latter is known to be sensitive for any local minima in the backscattering signal (Hennemuth and Lammert, 2006), which causes uncertainty especially during convective situations with turbulent aerosol mixing. The WCT technique analyzes the aerosol signatures of the lidar range-corrected signal profile. The covariance transform is a measure of the similarity of the range-corrected lidar signal and the related Haar function. The method was applied for the profiles measured with Polly<sup>XT</sup> following the guidelines introduced by Baars et al. (2008). In this study we applied the WCT method using 15 min averages of the measured backscatter signal at the wavelength of 1064 nm.

The results obtained from lidar data were used as the basis throughout the entire comparison period. The comparable hourly PBL top height value was calculated from lidar data using the average of the three closest data points of the hour considered. These PBL top height values were the basis for the comparison to other methods.

The daily PBL growth rates and growth periods were determined as described by Baars et al. (2008), i.e. the main growth period starts when the PBL height begins to

## Atmospheric boundary layer top height in South Africa

K. Korhonen et al.

Title Page

Abstract

Introduction

Conclusions

References

Tables

Figures

◀

▶

◀

▶

Back

Close

Full Screen / Esc

Printer-friendly Version

Interactive Discussion



increase (typically between 08:00 and 10:00 LT at the lidar site) and it ends when 90 % of the daily maximum height has been reached (typically between 16:00 and 18:00 LT). Then the growth rate was taken to be the slope of a linear fit to the data.

### 3.7.2 Radio soundings

We chose to determine the PBL top height by studying the height of surface-based inversion (Hanna, 1969; Keder, 1999; Seibert et al., 2000). The inversion was determined subjectively using measured vertical profiles of  $T$  and RH. This method is suitable for analysing small datasets including both day (convective conditions) and night (stable conditions with capping inversion on the top of PBL) soundings and can hence be applied for the dataset used in this study (409 soundings during 2010). There were two major periods in 2010 when radiosonde data was unavailable, i.e. 16 June–12 July and 3 August–17 October. The meteorological characteristics of the measurement site (Laakso et al., 2012) supported the choice of method with frequent strong temperature inversions, and thus, weak vertical mixing.

### 3.7.3 Models

The ECMWF model defines the PBL top height by using the bulk Richardson method with a critical Richardson number ( $Ri_{Cr}$ ) value of 0.25 (ECMWF, 2010b). If the  $Ri_{Cr}$  is detected between two vertical levels, linear interpolation is used for finding the PBL top height. This method combined with 62 vertical grid levels ensures high accuracy in modelling. The model gives the height of the stable boundary layer (SBL) in non-convective conditions, i.e. during times when the sun is below the horizon. Due to this characteristic we chose only day-time (08:00, 11:00, 14:00 and 17:00 LT) values for comparison with the lidar and radiosonde measurements. The PBL growth rates were determined from the slope of the linear fit to PBL heights between the first data point after sunrise (08:00 LT) and the point when the model indicated the daily maximum height (mostly at 17:00 LT).

## Atmospheric boundary layer top height in South Africa

K. Korhonen et al.

Title Page

Abstract

Introduction

Conclusions

References

Tables

Figures



Back

Close

Full Screen / Esc

Printer-friendly Version

Interactive Discussion







## Atmospheric boundary layer top height in South Africa

K. Korhonen et al.

Title Page

Abstract

Introduction

Conclusions

References

Tables

Figures

◀

▶

◀

▶

Back

Close

Full Screen / Esc

Printer-friendly Version

Interactive Discussion



Radiosonde measurements were obtained for 409 soundings on 200 separate days during 2010. Soundings were not available between 3 August 2010 and 18 October 2010. The SAWS model data covered the whole year and the PBL heights were calculated for the days when Polly<sup>XT</sup> was operational, i.e. 8 values for each day. The ECMWF model and the TAPM model produced 8 and 24 PBL top height values, respectively, for each day of 2010.

During 2010, 102 CALIPSO overpasses were available inside a  $2^\circ \times 2^\circ$  box centred on Elandsfontein. The minimum overpass distance was 60 km, while the maximum distance was 110 km from the lidar station. In 61 cases the boundary top location algorithm (SIBYL, Selective Iterated BoundarY Locator) identified at least one layer, while in 41 cases no layers could be identified. For this total of 61 cases, the PBL top from ground-based lidar was available for 29 cases. In those cases when two or more layers were observed, we considered the top of the first layer from the ground to be the PBL top height. However, in three cases, the top of the second layer is taken, since it is obvious from the attenuated backscatter image provided by CALIOP ([http://www.calipso.larc.nasa.gov/products/lidar/browse\\_images/production/](http://www.calipso.larc.nasa.gov/products/lidar/browse_images/production/)) that the first layer corresponds to a layer inside the PBL.

### 4.2 Diurnal PBL cycle

Figure 4 shows the annual average of diurnal PBL evolution for the common data points. The sunrise times varied between 05:07 and 06:56 LT, while sunset times ranged between 17:23 and 19:05 LT – these time are indicated with the shaded areas in Fig. 4. From the data presented differences between the approaches used to determine the PBL top height investigated in this study are observed. The lidar measurements cover both day-time CBL and nocturnal RL heights, similarly to the SAWS model. The ECMWF and TAPM models base their evaluation of PBL height on convective updraft strength, therefore producing low values during night-time. Radiosondes were launched from Pretoria at approximately 10:00 and 22:00 LT.



### 4.3 Annual PBL cycle

The PBL top daily maximum heights were studied for 174 days during 2010. In order to obtain a reliable determination of the daily maximum PBL top height, sufficient data coverage between 12:00 and 18:00 LT with neither wet removal of aerosols (rain) nor clouds inside the convectively mixed aerosol layer were utilised. Figure 5 shows the seasonal cyclic behaviour of the monthly average of the daily maximum PBL top heights. The annual PBL cycle can be clearly seen for all methods between March and October. November is a clear exception due to the low number of measurement days (three) caused by a maintenance break (Fig. 5). The relatively low average PBL top height value for December can be attributed to increased precipitation and cloudiness (205 h, i.e. 48.0% of the measurement time of cloudiness was observed with the Polly<sup>XT</sup>), and therefore less heating from the surface. Overall, the annual cyclic behaviour of PBL top heights follows the cycle of the solar radiation measured at the site (Fig. 2b).

It appears that TAPM produces systematically lower values for PBL top height throughout the year. It has to be noted that the ECMWF and SAWS modelled results may also underestimate the PBL top maximum height slightly due to the 3 h data resolution, i.e. the actual PBL maximum values may occur between the data points. Figure 6 shows the frequency distributions of all the daily maxima observed with the Polly<sup>XT</sup> and the models. As Fig. 6a, b shows the Polly<sup>XT</sup> and ECMWF model indicate only a slightly skewed normal distribution with medians of 1730 m and 1640 m PBL top height, respectively. TAPM (Fig. 6c) also gives a similarly skewed normal distribution, but the median of 1200 m is approximately 400–500 m lower. The SAWS model distribution (Fig. 6d) has a median value of 1420 m. There is also no uniform distribution due to the sparse vertical resolution of the data. The PBL top heights are distributed along the altitude levels of the model.

## Atmospheric boundary layer top height in South Africa

K. Korhonen et al.

Title Page

Abstract

Introduction

Conclusions

References

Tables

Figures



Back

Close

Full Screen / Esc

Printer-friendly Version

Interactive Discussion



## 4.4 Planetary boundary layer characteristics

This section summarizes the PBL characteristics determined with the Polly<sup>XT</sup> lidar for 2010 at Elandsfontein. The discussion of stable boundary layer (SBL) is based on the ECMWF and TAPM models. The presented features could be generalized to some extent for different years (the year 2010 average temperature was close to the long-term averages) in southern Africa in areas with similar surface properties and solar radiation. As shown in Fig. 5, the seasonal cycle of the PBL top height is explicit and follows the cycle of solar radiation (Fig. 2b). On average, the PBL top was highest in spring (September and October with heights of 2170 and 2260 m, respectively), while it was the lowest in winter (May–August with heights of 1450–1790 m) and in December (1210 m). As previously mentioned, the lower value in December was due to increased precipitation and cloudiness. The diurnal cycle is also well pronounced (Fig. 4). The evolution of the observed CBL started approximately 3 to 4 h after sunrise and the daily PBL top maximum was reached about 3.5 h after the solar noon. The models following the CBL (ECMWF and TAPM) show that the SBL top during night-time is on average 160 m (monthly averages varying from 70 to 270 m). The RL top (defined by the lidar) remains on average at 890 m during the night (monthly averages from 450 to 1370 m). The low SBL heights observed support earlier findings that indicated that the night-time domestic pollution is trapped near the surface of the earth surface and heavily impacts the local air quality (Venter et al., 2012). With the low SBL during the night, the industrial emissions from high stacks are most probably released and lifted to the RL, and thus their immediate effect on air quality during the night is smaller.

## 4.5 PBL growth rates

Figure 7 presents the PBL growth rates determined in 2010. All modelled values (Fig. 7b–d) are in relatively good agreement with the Polly<sup>XT</sup> measurements presented in Fig. 7a. The mode of the lidar, the ECMWF model (Fig. 7b) and the SAWS model (Fig. 7d) is 120–180 m h<sup>-1</sup> with frequencies of 34.0 %, 35.3 %, and 39.9 %, respectively.

## Atmospheric boundary layer top height in South Africa

K. Korhonen et al.

Title Page

Abstract

Introduction

Conclusions

References

Tables

Figures

◀

▶

◀

▶

Back

Close

Full Screen / Esc

Printer-friendly Version

Interactive Discussion



The corresponding median values for the lidar, the ECMWF model and the SAWS model are 183, 167 and 163  $\text{m h}^{-1}$ , respectively. The median of TAPM (Fig. 7c) at 172  $\text{m h}^{-1}$  agrees with the other methods although the deviation is greater with only 25.4% of the values in the range of 120–180  $\text{m h}^{-1}$ . The lower mode of TAPM, i.e. 60–120  $\text{m h}^{-1}$  with a frequency of 36.4% can partly explain the previous result of systematical underestimation of PBL top height values. Therefore the length of the growth period was typically similar to that of the Polly<sup>XT</sup> measurements with an average of 6.8 h (Polly<sup>XT</sup> 6.7 h).

### 4.6 Comparison of the PBL top height determination with different methods

The comparison was carried out for boundary layer evolution during convective conditions, i.e. when the sun was above the horizon (11:00–17:00 LT). The modelled PBL top heights were subtracted from those measured with the lidar. Figure 8a shows the monthly mean difference between each comparison for days when PBL maximum height was considered to be detected reliably with the lidar. The variability increased during the rainy season (October–March), which is evident for the strong anomaly observed during October. The increased variability is mainly due to the effect of increased cloudiness. The seasonal differences seem to have similar seasonal pattern for each of the models. Similar plots (Figs. 8b–d) are presented separately for the 11:00, 14:00 and 17:00 LT data points. In general, the differences between the methods are largest at 11:00 LT when mixing starts.

#### 4.6.1 Ground-based Lidar – Polly<sup>XT</sup>

As mentioned earlier, the lidar data set was selected as the base for the comparison due to its good temporal and vertical resolution. The drawbacks of the ground-based lidar are associated with the technical complexity of the instrument, sensitivity for rain and complex aerosol structures. Still, the PBL top height was detected in about 86% of all the measurement data (42% of the total time). In general, the lidar data has more

variation during the rainy season, which may partly explain the large differences observed in October. The maintenance was carried out during the rainy season resulting in a smaller dataset, which can also partly explain the uncertainties. The time delay tests showed that the lidar observes the start of the boundary layer evolution a bit later than the ECMWF model. Comparing to other methods used, this time delay did not increase the correlation.

#### 4.6.2 ECMWF

The ECMWF model shows the best correlation to lidar measurements with only 15.4 % mean absolute difference, when October is excluded from the comparison. Half of the ECMWF PBL top values (51 %) are within  $\pm 20\%$ , while 81 % are within  $\pm 50\%$  of the lidar values. When comparing only the PBL top height at 14:00 LT the corresponding values are 61 % and 90 %. The ECMWF model tends to evaluate the PBL top a bit higher than the PBL top measured with the Polly<sup>XT</sup> (in 63 % of the cases). A clear seasonal pattern is observed in differences between the two methods (Fig. 8). The best agreement is found between March and July, i.e. during the dry season. A plausible explanation for this is the similar pattern observed in global radiation (GR) daily maxima (see Fig. 2b). The PBL top evaluation by the ECMWF model is based on the strength of convection, and therefore the model is sensitive to changes in GR. The monthly averages of daily maximum GR decrease strongly during autumn from  $1000 \text{ W m}^{-2}$  in March to  $760 \text{ W m}^{-2}$  in April. The average daily maximum intensity remains below  $800 \text{ W m}^{-2}$  until September, after which it increases to  $920 \text{ W m}^{-2}$  and further increases to above  $1000 \text{ W m}^{-2}$  for the rest of the year.

#### 4.6.3 TAPM

Comparison between Polly<sup>XT</sup> and TAPM indicates systematic underestimation of PBL top height by the model, with all months showing higher values for the Polly<sup>XT</sup> measurements. The mean absolute difference in the comparison between the lidar and TAPM is

### Atmospheric boundary layer top height in South Africa

K. Korhonen et al.

Title Page

Abstract

Introduction

Conclusions

References

Tables

Figures

◀

▶

◀

▶

Back

Close

Full Screen / Esc

Printer-friendly Version

Interactive Discussion



## Atmospheric boundary layer top height in South Africa

K. Korhonen et al.

Title Page

Abstract

Introduction

Conclusions

References

Tables

Figures

◀

▶

◀

▶

Back

Close

Full Screen / Esc

Printer-friendly Version

Interactive Discussion



34.7 %. The modelled values are smaller than PBL top heights measured with the lidar for 92 % of the cases. This is also observed by comparing TAPM to the other models. TAPM model values are smaller than the ECMWF PBL top height values for 95 % of the cases. A different seasonal behaviour is observed compared to the lidar and to the ECMWF model (Fig. 8). In a similar way as the ECMWF model, TAPM estimates the PBL height through the strength of convection and the differences to the lidar measurement indicate that increasing GR intensity improves the performance of the model. Hence, the differences compared to the lidar measurements are significantly lower in warmer months (October–February). However, the number of measurement days was low in January and November with only five and three days, respectively. Just 16 % of the TAPM PBL top height values are within  $\pm 20\%$  and 60 % are within  $\pm 50\%$  of the lidar values. When comparing TAPM with the ECMWF model, the corresponding ( $\pm 20\%$  and  $\pm 50\%$ ) values were 9 % and 40 %.

In order to explain the differences observed, the model temperature, radiation and wind speed were compared to the ground-based measurements. The model temperature and GR compared well with the measurements. The mean absolute difference in temperature values between the model and measurements was about 4 %. Nevertheless, the model underestimates the wind speed significantly. The mean absolute difference was 23 % and 60 % of the model wind speeds were within  $\pm 50\%$  of the measured values. About 74 % of the model values were smaller than the measured wind speed. The underestimation of the wind speed probably leads to underestimation of the vertical wind and turbulence and thus underestimating the PBL top height. This may partly explain the observed differences.

### 4.6.4 SAWS

The SAWS operated model shows the second best correlation with a mean absolute difference of 20.1 % during day-time. About 35 % of the SAWS PBL top values are within  $\pm 20\%$ , while 78 % are within  $\pm 50\%$  of the lidar values. When comparing only the PBL at 14:00 LT, the corresponding values are 40 % and 83 %. Unlike other mod-

## Atmospheric boundary layer top height in South Africa

K. Korhonen et al.

Title Page

Abstract

Introduction

Conclusions

References

Tables

Figures

◀

▶

◀

▶

Back

Close

Full Screen / Esc

Printer-friendly Version

Interactive Discussion



els, the SAWS model does not show a clear seasonal difference in comparison to the Polly<sup>XT</sup> lidar. The SAWS model values were lower than the lidar values in 78 % of the cases and smaller than the ECMWF values in 85 % of the cases. The systematic variation is mostly due to the relatively low vertical resolution of the model (16 levels) with fixed pressure levels. Therefore, the vertical resolution is a few hundred metres in the lowermost troposphere and may cause large bias on PBL top height estimation. However, the averages are relatively close to the lidar results.

The model temperature and wind speed were compared to the ground-based measurements. The model temperature compared reasonably well to the measurements, with the mean absolute difference being about 8 %. Nevertheless, the SAWS model also tends to underestimate the wind speed. The mean absolute difference in the wind speed was 46 % and 45 % of the model wind speeds were within  $\pm 50$  % of the measured values. In addition, about 89 % of the model values were smaller than the measured wind speed. Due to the method used to determine the PBL top height, the relation of wind speed to the PBL height is not obvious. Notwithstanding the underestimation of the wind speed may affect the higher altitude weather parameters in the model and therefore have consequences for the PBL top height determination.

### 4.6.5 Radio soundings

The radiosonde launch site (Pretoria) is 120 km from the lidar site, which may explain some of the observed differences in addition to the robust and manual method in defining the PBL top value. The comparison was carried out by calculating correlations between the results from each method and the radiosonde observations. For comparisons including ECMWF and TAPM models we chose only the morning soundings that were carried out in convective conditions (sun above horizon). For the comparison between the Polly<sup>XT</sup> and the SAWS model, both morning and evening soundings were used.

The PBL top heights derived from the radiosonde observations tend to show higher values than the top heights from Polly<sup>XT</sup> (in 81 % of the cases). The deviation is large

---

## Atmospheric boundary layer top height in South Africa

K. Korhonen et al.

---

Title Page

Abstract

Introduction

Conclusions

References

Tables

Figures

◀

▶

◀

▶

Back

Close

Full Screen / Esc

Printer-friendly Version

Interactive Discussion



throughout the comparison period (Fig. 9a). About 30 % of the sounding derived PBL top values were within  $\pm 20$  % and 60 % were within  $\pm 50$  % of the lidar PBL top values. For the overall comparison, the slope of the fit is 0.68 (x-intercept forced to zero in all fittings) with a correlation coefficient ( $R$ ) of 0.54. The total number of simultaneous observations is 133. We found that the discrepancy between the PBL tops based on lidar measurements and radio soundings is larger in convective conditions (comparison between all 67 day-time soundings: slope 0.66,  $R$  0.41) than during night-time (66 soundings), when the slope of the fit remains roughly the same (0.69) but  $R$  increases to 0.61.

The correlation between the ECMWF model and the radiosondes is presented in Fig. 9b. The fit shows radiosonde measurements have larger PBL heights with the slope of the linear fit being 0.89 and  $R$  being 0.53. The results show that the soundings give smaller PBL top values in 69 % of the cases and 25 % of the values are within  $\pm 20$  % and 57 % are within  $\pm 50$  % of the ECMWF model values. The values for TAPM (slope/ $R$ ) are 0.25/0.14 and for the SAWS model 0.57/0.47 (Fig. 9c and d, respectively). Figure 9d shows the distribution of the SAWS model results which are grouped together at fixed heights due to the coarse pressure level resolution of the model (see also Fig. 6d).

### 4.6.6 Space-borne lidar

Comparisons of PBL top heights between ground-based Polly<sup>XT</sup> lidar and space-borne CALIOP lidar have been performed for the 29 common cases. The CALIOP overpasses were between 60 and 110 km from the lidar site. The scatter plot between CALIOP and Polly<sup>XT</sup> lidar derived PBL heights shows a good correlation with a correlation coefficient of 0.88 (Fig. 10). The majority of our data accounts for PBL heights lower than 3 km. Neither the distance between the overpass and the lidar station nor the time difference seems to affect our comparison. The overestimation seems to be larger for larger PBL top heights.

## 5 Comparison to other locations

This study is the first long term study of PBL top heights and PBL growth rates in the Southern Hemisphere. Only a few studies have been performed in Europe and Asia, most of them with less data coverage.

The average PBL top height under convective conditions (08:00–17:00 LT) at  $1.4 \pm 0.5$  km AGL is comparably high, with its highest values and variability in spring ( $1.6 \pm 0.7$  km) and lower values in the other seasons (1.3 km). Within Europe, maximum values occurred during summer, e.g. 1.8 km in Leipzig, Germany (Baars et al., 2008) and 1.3 km in Granada, Spain (Granados-Muñoz et al., 2012). In winter both of these studies showed values around 0.8 km. Chen et al. (2001) have reported PBL top heights of 1.0 km for a site in Japan in spring and autumn, while PBL top heights were 0.4 and 0.7 km in winter and summer, respectively. Hänel et al. (2012) have reported night-time PBL top heights of 0.7 to 1.1 km in the vicinity of Beijing, China, with maximum values in spring and summer.

According to PBL growth rates, the values found in this study compare well with other locations and maximum values coincide with the maximum PBL top heights. PBL growth rates were, thus, highest in spring with  $220 \pm 100$   $\text{m h}^{-1}$  and lower during the other seasons. On average, growth rates between 100 and 300 m were found. Baars et al. (2008) found growth rates of 100 to 300  $\text{m h}^{-1}$  most of the year and 400 to 500  $\text{m h}^{-1}$  in summer. Chen et al. (2001) reported lower growth rates of 30 to 100  $\text{m h}^{-1}$  with peak values of 140  $\text{m h}^{-1}$  in autumn.

## 6 Summary and conclusions

One year of PBL top height observations done with Polly<sup>XT</sup> lidar were compared with three atmospheric models, radio soundings and CALIOP space-borne lidar in SA. It was shown that the lidar is suitable for continuous measurements. We had data coverage of 49 % for the complete sampling period (60 % if maintenance breaks are ex-

### Atmospheric boundary layer top height in South Africa

K. Korhonen et al.

Title Page

Abstract

Introduction

Conclusions

References

Tables

Figures

◀

▶

◀

▶

Back

Close

Full Screen / Esc

Printer-friendly Version

Interactive Discussion



---

## Atmospheric boundary layer top height in South Africa

K. Korhonen et al.

---

Title Page

Abstract

Introduction

Conclusions

References

Tables

Figures

◀

▶

◀

▶

Back

Close

Full Screen / Esc

Printer-friendly Version

Interactive Discussion



cluded). For the lidar PBL top height determination the WCT method performed well despite frequent complex vertical aerosol layer structures caused by large emissions from large point sources and biomass burning. The lidar detected the PBL top height for 86 % of all the measurements (42 % of the total time). The best performance in data coverage and PBL height detection was observed during the dry season (April–September), when rain and cloudy conditions had only a minor impact on the measurements and aerosol concentrations were the highest.

The comparison between Polly<sup>XT</sup> lidar and radiosonde measurements showed large variation. The method in PBL determination from radio soundings consists of finding the altitude of surface-based temperature inversion and it produced better correlation with the lidar during night-time (RL), when temperature inversions were more evident. However, also the distance between the radio sounding and the lidar location may have led to the observed differences. Despite their limitations in temporal resolution and PBL top height determination uncertainty, radio soundings have been routinely used for decades and therefore are a valuable method for long-term climatology analyses.

The results from the ECMWF model indicated the best agreement with the lidar data in the annual PBL cycle. Hence, the model predicts the daily PBL top maximum height well despite its 3 h temporal resolution. In addition, the PBL growth rates agree well with those derived from lidar data. The performance of the model is the best during the dry season (May–June) with relatively small average overestimation (8.2 %) of PBL top height when all day-time values (11:00, 14:00 and 17:00 LT) are compared with the Polly<sup>XT</sup> data. During spring and summer (October–February) the differences varied more, which is most probably a combined result from weather-related limitations of lidar measurements leading to smaller data set.

The SAWS model performed well in general, regarding the fixed pressure levels with 50 hPa intervals, which results in vertical resolution of about 500 m near surface. The model performs second-best with regard to day-time PBL top height evaluation with only slightly larger mean absolute difference to the lidar measurements (20.1 %). Similar uncertainties were observed as for the radio soundings, but the overall perfor-



depending on the model grid (even though it was centred at our site). If the PBL top heights are used in air quality modelling, the possible unrealistic PBL top height variations will be transferred directly to the air quality results through aerosol vertical mixing. More direct measurements of the PBL top heights e.g. with lidars could be used to verify the models.

*Acknowledgements.* This work has been partly supported by the European Union (in project EUCAARI). The authors acknowledge the staff of the North-West University for valuable assistance and routine maintenance of the lidar. We also acknowledge Eskom and Sasol for their logistical support for measurements at Elandsfontein.

## References

- Althausen, D., Engelmann, R., Baars, H., Heese, B., Ansmann, A., Müller, D. and Komppula, M.: Portable raman lidar pollyxt for automated profiling of aerosol backscatter, extinction, and depolarization, *J. Atmos. Ocean. Tech.*, 26, 2366–2378, 2009.
- Amiridis, V., Melas, D., Balis, D. S., Papayannis, A., Founda, D., Katragkou, E., Giannakaki, E., Mamouri, R. E., Gerasopoulos, E., and Zerefos, C.: Aerosol Lidar observations and model calculations of the Planetary Boundary Layer evolution over Greece, during the March 2006 Total Solar Eclipse, *Atmos. Chem. Phys.*, 7, 6181–6189, doi:10.5194/acp-7-6181-2007, 2007.
- Ansmann, A., Baars, H., Tesche, M., Müller, D., Althausen, D., Engelmann, R., Pauliquevis, T., and Artaxo, P.: Dust and smoke transport from Africa to South America: lidar profiling over Cape Verde and the Amazon rainforest, *Geophys. Res. Lett.*, 36, L11802, doi:10.1029/2009GL037923, 2009.
- Baars, H., Ansmann, A., Engelmann, R., and Althausen, D.: Continuous monitoring of the boundary-layer top with lidar, *Atmos. Chem. Phys.*, 8, 7281–7296, doi:10.5194/acp-8-7281-2008, 2008.
- Brooks, I. M.: Finding boundary layer top: application of a wavelet covariance transform to lidar backscatter profiles, *J. Atmos. Ocean. Tech.*, 20, 1092–1195, 2003.
- Campbell, J. R., Welton, E., Spinhirne, J. D., Ji, Q., Tsay, S. C., Piketh, S. P., and Barenbrug, M.: Micropulse lidar observations of tropospheric aerosols over northeastern South Africa during

## Atmospheric boundary layer top height in South Africa

K. Korhonen et al.

Title Page

Abstract

Introduction

Conclusions

References

Tables

Figures

◀

▶

◀

▶

Back

Close

Full Screen / Esc

Printer-friendly Version

Interactive Discussion



---

**Atmospheric  
boundary layer top  
height in South Africa**K. Korhonen et al.

---

[Title Page](#)[Abstract](#)[Introduction](#)[Conclusions](#)[References](#)[Tables](#)[Figures](#)[◀](#)[▶](#)[◀](#)[▶](#)[Back](#)[Close](#)[Full Screen / Esc](#)[Printer-friendly Version](#)[Interactive Discussion](#)

the ARREX and SAFARI 2000 dry season experiments, *J. Geophys. Res.*, 108, 8497–8530, doi:10.1029/2002JD002563, 2003.

Chen, W., Kuze, H., Uchiyama, A., Suzuki, Y., and Takeuchi, N.: One-year observation of urban mixed layer characteristics at Tsukuba, Japan using a micro pulse lidar, *Atmos. Environ.*, 35, 4273–4280, ISSN 1352-2310, doi:10.1016/S1352-2310(01)00181-9, 2001.

Derbyshire, S. H.: Nieuwstadt's stable boundary layer revisited, *Q. J. Roy. Meteorol. Soc.*, 116, 127–158, 1990.

ECMWF: IFS Documentation – Cy36r1, Part 5: Ensemble prediction system, ECMWF, 2010a.

ECMWF: IFS Documentation – Cy36r1, Part 4: Physical processes, ECMWF, 2010b.

Formenti, P., Winkler, H., Fourie, P., Piketh, S., Makgopa, B., Helas, G., and Andreae, M. O.: Aerosol optical depth over a remote semi-arid region of South Africa from spectral measurements of the daytime solar extinction and the nighttime stellar extinction, *Atmos. Res.*, 62, 11–32, doi:10.1016/S0169-8095(02)00021-2, 2002.

Formenti, P., Elbert, W., Maenhaut, W., Haywood, J., S. Osborne, and Andreae, M. O.: Inorganic and carbonaceous aerosols during the Southern African Regional Science Initiative (SAFARI 2000) experiment: Chemical characteristics, physical properties, and emission data for smoke from African biomass burning, *J. Geophys. Res.*, 108, D138488, doi:10.1029/2002JD002408, 2003.

Garratt, J. R.: *The Atmospheric Boundary Layer*, Cambridge University Press, ISBN: 0-521-38052-9, 1992.

Granados-Muñoz, M. J., Navas-Guzmán, F., Bravo-Aranda, J. A., Guerrero-Rascado, J. L., Lyamani, H., Fernandez-Galvez, J., and Alados-Arboledas, L.: Automatic determination of the planetary boundary layer height using lidar: one-year analysis over Southeastern Spain., *J. Geophys. Res.*, 117, D18208, doi:10.1029/2012JD017524, 2012.

Groß, S., Gasteiger, J., Freudenthaler, V., Wiegner, M., Geiß, A., Schladitz, A., Toledano, C., Kandler, K., Tesche, M., Ansmann, A., and Wiedensohler, A.: Characterization of the planetary boundary layer during SAMUM-2 by means of lidar measurements, *Tellus B*, 63, 695–705, doi:10.1111/j.1600-0889.2011.00557.x, 2011.

Hanna, S. R.: The thickness of the planetary boundary layer, *Atmos. Environ.*, 3, 519–536, doi:10.1016/0004-6981(69)90042-0, 1969.

Hennemuth, B. and Lammert, A.: Determination of the atmospheric boundary layer height from radiosonde and lidar backscatter, *Bound.-Lay. Meteorol.*, 120, 181–200, doi:10.1007/s10546-005-9035-3, 2006.

## Atmospheric boundary layer top height in South Africa

K. Korhonen et al.

Title Page

Abstract

Introduction

Conclusions

References

Tables

Figures

◀

▶

◀

▶

Back

Close

Full Screen / Esc

Printer-friendly Version

Interactive Discussion



- Hurley, P.: TAPM V4. Part 1: Technical description, CSIRO marine and atmospheric research paper No. 25, October 2008, ISBN: 978-1-921424-71-7, 2008.
- Hurley, P. J., Physick, W. L., and Luhar, A. K.: TAPM: a practical approach to prognostic meteorological and air pollution modelling, *Environ. Modell. Softw.*, 20, 737–752, 2005a.
- 5 Hurley, P. J., Physick, W., Luhar, A., and Edwards, M.: The Air Pollution Model (TAPM) Version 3, Part 2: Summary of some verification studies, CSIRO, *Atmos. Res.*, 72, 20–36, 2005b.
- Hurley, P. J., Edwards, M., and Luhar, A.: TAPM V4, Part 2: Summary of some verification studies, CSIRO marine and atmospheric research paper No. 26, October 2008, ISBN: 978-1-921424-72-4, 2008.
- 10 Hänel, A., Baars, H., Althausen, D., Ansmann, A., Engelmann, R., and Sun, J. Y.: One-year aerosol profiling with EUCAARI Raman lidar at Shangdianzi GAW station: Beijing plume and seasonal variations, *J. Geophys. Res.*, 117, D13201, doi:10.1029/2012JD017577, 2012.
- Johansson, C. and Bergström H.: An auxiliary tool to determine the height of the boundary layer, *Bound.-Lay. Meteorol.*, 115, 423–432, doi:10.1007/s10546-004-1424-5, 2005.
- 15 Jordan, N. S., Hoff, R. M., and Bacmeister, J. T.: Validation of Goddard Earth Observing System-version 5 MERRA planetary boundary layer heights using CALIPSO, *J. Geophys. Res.*, 115, D24218, doi:10.1029/2009JD013777, 2010.
- Keder, J.: Detection of inversions and mixing height by REMTECH PA2 sodar in comparison with collocated radiosonde measurements, *Meteorol. Atmos. Phys.*, 71, 133–138, 1999.
- 20 Kulmala, M., Asmi, A., Lappalainen, H. K., Baltensperger, U., Brenguier, J.-L., Facchini, M. C., Hansson, H.-C., Hov, Ø., O'Dowd, C. D., Pöschl, U., Wiedensohler, A., Boers, R., Boucher, O., de Leeuw, G., Denier van der Gon, H. A. C., Feichter, J., Krejci, R., Laj, P., Lihavainen, H., Lohmann, U., McFiggans, G., Mentel, T., Pilinis, C., Riipinen, I., Schulz, M., Stohl, A., Swietlicki, E., Vignati, E., Alves, C., Amann, M., Ammann, M., Arabas, S., Artaxo, P., Baars, H.,
- 25 Beddows, D. C. S., Bergström, R., Beukes, J. P., Bilde, M., Burkhardt, J. F., Canonaco, F., Clegg, S. L., Coe, H., Crumeyrolle, S., D'Anna, B., Decesari, S., Gilardoni, S., Fischer, M., Fjaeraa, A. M., Fountoukis, C., George, C., Gomes, L., Halloran, P., Hamburger, T., Harrison, R. M., Herrmann, H., Hoffmann, T., Hoose, C., Hu, M., Hyvärinen, A., Hörrak, U., Iinuma, Y., Iversen, T., Josipovic, M., Kanakidou, M., Kiendler-Scharr, A., Kirkevåg, A.,
- 30 Kiss, G., Klimont, Z., Kolmonen, P., Komppula, M., Kristjánsson, J.-E., Laakso, L., Laaksonen, A., Labonnote, L., Lanz, V. A., Lehtinen, K. E. J., Rizzo, L. V., Makkonen, R., Manninen, H. E., McMeeking, G., Merikanto, J., Minikin, A., Mirme, S., Morgan, W. T., Nemitz, E., O'Donnell, D., Panwar, T. S., Pawlowska, H., Petzold, A., Pienaar, J. J., Pio, C.,

## Atmospheric boundary layer top height in South Africa

K. Korhonen et al.

Title Page

Abstract

Introduction

Conclusions

References

Tables

Figures

◀

▶

◀

▶

Back

Close

Full Screen / Esc

Printer-friendly Version

Interactive Discussion

Plass-Duelmer, C., Prévôt, A. S. H., Pryor, S., Reddington, C. L., Roberts, G., Rosenfeld, D., Schwarz, J., Seland, Ø., Sellegri, K., Shen, X. J., Shiraiwa, M., Siebert, H., Sierau, B., Simpson, D., Sun, J. Y., Topping, D., Tunved, P., Vaattovaara, P., Vakkari, V., Veefkind, J. P., Visschedijk, A., Vuollekoski, H., Vuolo, R., Wehner, B., Wildt, J., Woodward, S., Worsnop, D. R., van Zadelhoff, G.-J., Zardini, A. A., Zhang, K., van Zyl, P. G., Kerminen, V.-M., Carslaw, K., and Pandis, S. N.: General overview: European Integrated project on Aerosol Cloud Climate and Air Quality interactions (EUCAARI) – integrating aerosol research from nano to global scales, *Atmos. Chem. Phys.*, 11, 13061–13143, doi:10.5194/acp-11-13061-2011, 2011.

Laakso, L., Vakkari, V., Virkkula, A., Laakso, H., Backman, J., Kulmala, M., Beukes, J. P., van Zyl, P. G., Tiitta, P., Josipovic, M., Pienaar, J. J., Chiloane, K., Gilardoni, S., Vignati, E., Wiedensohler, A., Tuch, T., Birmili, W., Piketh, S., Collett, K., Fourie, G. D., Komppula, M., Lihavainen, H., de Leeuw, G., and Kerminen, V.-M.: South African EUCAARI measurements: seasonal variation of trace gases and aerosol optical properties, *Atmos. Chem. Phys.*, 12, 1847–1864, doi:10.5194/acp-12-1847-2012, 2012.

Lai, L. and Cheng, W. L.: Air quality influenced by urban heat island coupled with synoptic weather patterns, *Sci. Total. Environ.*, 4, 2724–2733, 2009.

Liu, L., Improving GCM Aerosol Climatology using satellite and ground based measurements, paper presented at 15th ARM Science Team Meeting, Atmos. Radiat. Meas. (ARM) Program, Daytona Beach, Fla., 14–18 March, 2005.

Liu, Z., Winker, D., Omar, A., Vaughan, M., Trepte, C., Hu, Y., Powell, K., Sun, W., and Lin, B.: Effective lidar ratios of dense dust layers over North Africa derived from the CALIOP measurements, *J. Quant. Spectrosc. Radiat. T.*, 112, 204–213, 2011.

Lourens, A. S. M., Beukes, J. P., van Zyl, P. G., Fourie, G. D., Burger, J. W., Pienaar, J. J., Read, C. E., and Jordaan, J. H. L.: Spatial and Temporal assessment of Gaseous Pollutants in the Mpumalanga Highveld of South Africa, *S. Afr. J. Sci.*, 107, 269, doi:10.4102/sajs.v107i1/2.269, 2011.

Lourens, S. M., Butler, T. M., Beukes, J. P., van Zyl, P. G., Beirle, S., Wagner, T., Heue, K.-P., Pienaar, J. J., Fourie, G. D., and Lawrence, M. G.: Re-evaluating the NO<sub>2</sub> hotspot over the South African Highveld, *S. Afr. J. Sci.*, 108, 1146, doi:10.4102/sajs.v108i11/12.1146, 2012.

Luhar, A.K and Hurley, P. J.: Application of a prognostic model TAPM to sea-breeze flows, surface concentrations, and fumigating plumes, *Environ. Modell. Softw.*, 19, 591–601, 2004.

## Atmospheric boundary layer top height in South Africa

K. Korhonen et al.

Title Page

Abstract

Introduction

Conclusions

References

Tables

Figures

◀

▶

◀

▶

Back

Close

Full Screen / Esc

Printer-friendly Version

Interactive Discussion

- Müller, D., Wandinger, U., Althausen, D., and Fiebig, M.: Comprehensive particle characterization from three-wavelength Raman-lidar observations: case study, *Appl. Optics*, 40, 4863–4869, 2001.
- 5 Pal, S. R., Steinbrecht, W., and Carswell, A. I.: Automated method for lidar determination of cloud base height and vertical extent, *Appl. Optics*, 31, 1488–1494, 1992.
- Piketh, S. J., Annegarn, H. J., and Tyson, P. D.: Lower tropospheric aerosol loadings over South Africa: the relative contribution of aeolian dust, industrial emissions, and biomass burning, *J. Geophys. Res.*, 104, 1597–1607, doi:10.1029/1998JD100014, 1999.
- 10 Piketh, S. J., Swap, R. J., W. Maenhaut, Annegarn, H. J., and Formenti, P.: Chemical evidence of long-range atmospheric transport over southern Africa, *J. Geophys. Res.*, 107, 4817, doi:10.1029/2002JD002056, 2002.
- Preston-Whyte, R. A. and Tyson, P. D.: *The Atmosphere and Weather of Southern Africa*, Oxford University Press, Cape Town, 1988.
- 15 Queface, A. J., Piketh, S. J., Eck, T. F., Tsay, S. C., and Mavume, A. F.: Climatology of aerosol optical properties in Southern Africa, *Atmos. Environ.*, 45, 2910–2921, 2011.
- Ragunandan, A., Scott, G., Zunckel, M., and Carter, W.: TAPM verification in South Africa: modelling surface meteorology at Alexander Bay and Richards Bay, Report done on behalf CSIR Natural Resources and the Environment, Congella, 2008.
- Schulze, B. R.: *Climate of South Africa*, Report no. WB 28, done on behalf of Department of Environment Affairs, Pretoria, 1965.
- 20 Seibert, P., Beyrich, F., Gryning, S.-E., Joffre, S., Rasmussen, A., and Teci, P.: Review and intercomparison of operational methods for the determination of the mixing height, *Atmos. Environ.*, 34, 1001–1027, 2000.
- Seidel, D. J., Zhang, Y., Beljaars, A., Golaz, J.-C., Jacobson, A. R., and Medeiros, B.: Climatology of the planetary boundary layer over the continental United States and Europe. *J. Geophys. Res.*, 117, D17106, doi:10.1029/2012JD018143, 2012.
- 25 Stull, R. B.: *An Introduction to Boundary Layer Meteorology*, Kluwer Academic Publishers, ISBN: 90-277-2768-6, 1988.
- Tyson, P. D., Garstang, M., Swap, R. J., Edwards, M., and Kallberg, P.: An air transport climatology for subtropical southern Africa, *Int. J. Climatol.*, 16, 265–291, 1996.
- Vaughan, M.A, Winker, D. M., and Powell, K. A.: CALIOP Algorithm Theoretical Basis Document Part 2: Feature Detection and Layer Properties Algorithms, available at: <http://>

//www-calipso.larc.nasa.gov/resources/pdfs/PC-SCI-202\_Part2\_rev1x01.pdf (last access: June 2013), 2005.

Venter, A. D., Vakkari, V., Beukes, J. P., van Zyl, P. G., Laakso, H., Mabaso, D., Tiitta, P., Josipovic, M., Kulmala, M., Pienaar, J. J., and Laakso, L.: An air quality assessment in the industrialised western Bushveld Igneous Complex, South Africa, *S. Afr. J. Sci.*, 108, 84–93, doi:10.4102/sajs.v108i9/10.1059, 2012.

Winker, D. M., Hunt, W. H., and McGill, M. J.: Initial performance assessment of CALIOP, *Geophys. Res. Lett.*, 34, L19803, doi:10.1029/2007GL030135, 2007.

Winker, D. M., Hostetler, C., and Hunt, W.: CALIOP: The CALIPSO Lidar, *Proc. 22nd International Laser Radar Conference (ESASP 561)*, Matera, Italy, 941–944, 2004.

Winker, D. M., Vaughan, M., and Hunt, W.: The CALIPSO mission and initial results from CALIOP, *Proc. SPIE*, 6409 (SPIE, Bellingham, WA 2006), 640902, doi:10.1117/12.698003, 2006.

Zawar-Reza, P. and Sturman, A.: Application of airshed modelling to the implementation of the New Zealand National Environmental Standards for air quality, *Atmos. Environ.*, 42, 8785–8794, 2008.

## ACPD

13, 17407–17450, 2013

### Atmospheric boundary layer top height in South Africa

K. Korhonen et al.

Title Page

Abstract

Introduction

Conclusions

References

Tables

Figures

⏪

⏩

◀

▶

Back

Close

Full Screen / Esc

Printer-friendly Version

Interactive Discussion



## Atmospheric boundary layer top height in South Africa

K. Korhonen et al.

**Table 1.** The main properties of the methods used in this study.

Method	Temporal resolution	Vertical resolution & range	Horizontal grid resolution	PBL types included	PBL height determination method
Polly <sup>XT</sup>	15 min (adjustable)	30 m (0–25 km or more)	point measurement	CBL + RL	Maximum mixing height via aerosol layer top height
Radiosonde	12 h	min. 50 m (up to ca. 20 km)	point measurement	CBL + RL	Manual detection of inversion height in $T$ & RH profiles
ECMWF	3 h	62 levels (highest level 5 hPa, typ. at ca. 45 km)	0.2° (~ 20 km)	CBL + SBL	Bulk Richardson number ( $Ri_{Cr} = 0.25$ )
SAWS (UM, SA domain archive)	1 h*	16 levels (850–100 hPa, typ. at ca. 16 km)	12 km	CBL + RL	Manual detection of inversion height in $T$ & RH profiles
TAPM	1 h	44 levels (0–4 km, adjustable)	1 km (adjustable)	CBL + SBL	Convective updraft strength
CALIOP	16 day repeat cycle	30 m	5 km	CBL + RL	Feature Detection and Layer Properties Algorithm

\* A temporal resolution of three hours was chosen for the SAWS model used in this study to correspond to the ECMWF model.

Title Page

Abstract

Introduction

Conclusions

References

Tables

Figures

◀

▶

◀

▶

Back

Close

Full Screen / Esc

Printer-friendly Version

Interactive Discussion



## Atmospheric boundary layer top height in South Africa

K. Korhonen et al.

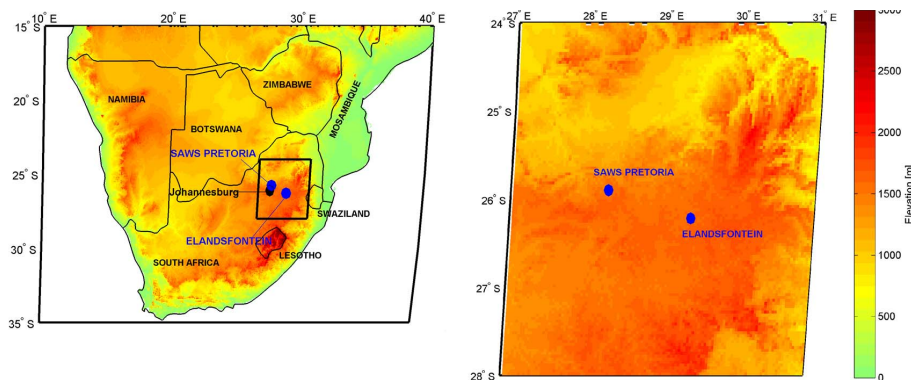


**Fig. 1.** Location of measurement site and the orographic information of the surroundings. The Elandsfontein lidar site was located 150 km east from Johannesburg. The map shows the location of the Pretoria sounding station 120 km from the lidar site.

[Title Page](#)[Abstract](#)[Introduction](#)[Conclusions](#)[References](#)[Tables](#)[Figures](#)[◀](#)[▶](#)[◀](#)[▶](#)[Back](#)[Close](#)[Full Screen / Esc](#)[Printer-friendly Version](#)[Interactive Discussion](#)

## Atmospheric boundary layer top height in South Africa

K. Korhonen et al.

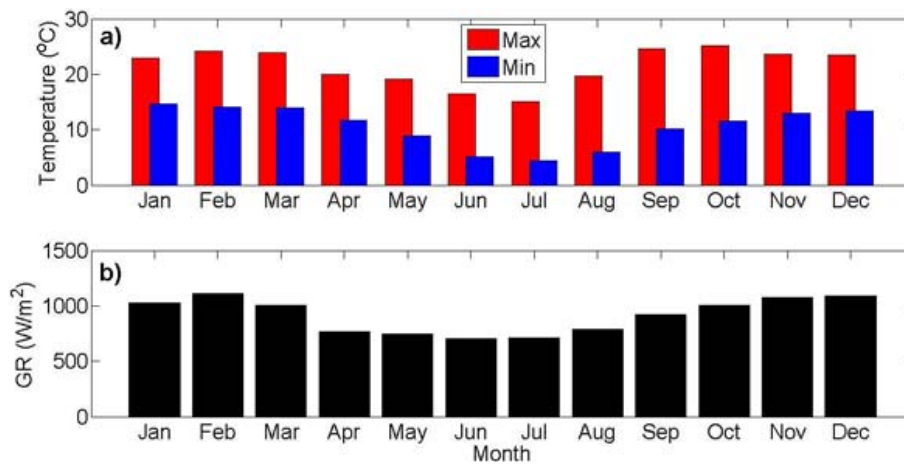


**Fig. 2.** Measured average temperatures **(a)** and daily maximum global radiation intensity **(b)** at Elandsfontein during 2010. In **(a)** the red bars indicate daily average maximum and blue bars the daily average minimum temperature. The values were calculated from 15 min averages.

[Title Page](#)[Abstract](#)[Introduction](#)[Conclusions](#)[References](#)[Tables](#)[Figures](#)[◀](#)[▶](#)[◀](#)[▶](#)[Back](#)[Close](#)[Full Screen / Esc](#)[Printer-friendly Version](#)[Interactive Discussion](#)



## Atmospheric boundary layer top height in South Africa

K. Korhonen et al.

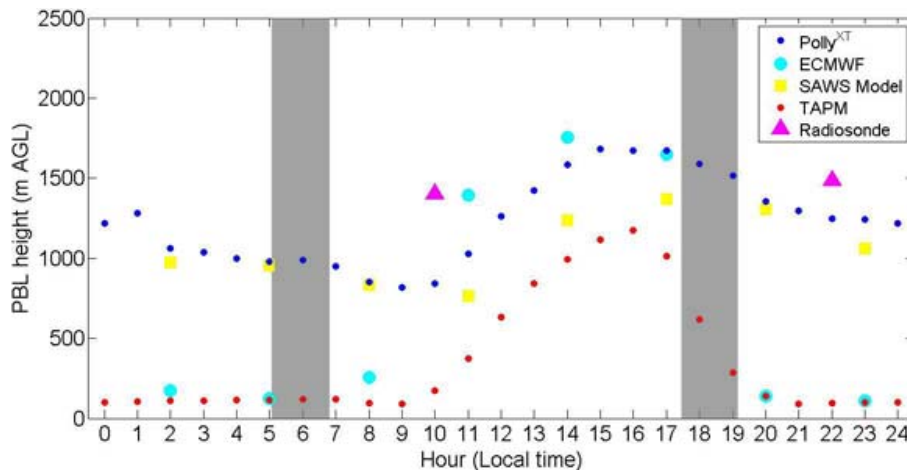


**Fig. 4.** PBL diurnal cycle observed in Elandsfontein during 2010. The grey shading indicates the times of sunrise and sunset.

[Title Page](#)[Abstract](#)[Introduction](#)[Conclusions](#)[References](#)[Tables](#)[Figures](#)[⏪](#)[⏩](#)[◀](#)[▶](#)[Back](#)[Close](#)[Full Screen / Esc](#)[Printer-friendly Version](#)[Interactive Discussion](#)

## Atmospheric boundary layer top height in South Africa

K. Korhonen et al.

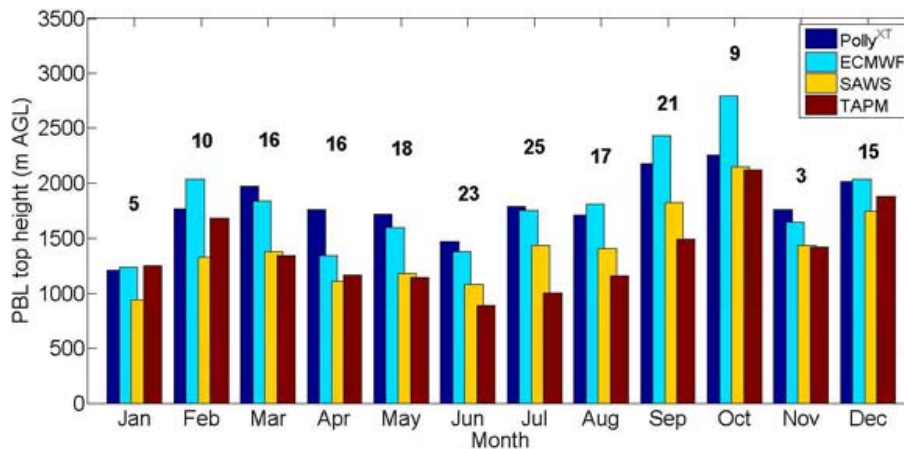


**Fig. 5.** Monthly averages of PBL daily maximum values. Numbers above bars indicate the number of measurement days on each month.

Title Page

Abstract

Introduction

Conclusions

References

Tables

Figures

◀

▶

◀

▶

Back

Close

Full Screen / Esc

Printer-friendly Version

Interactive Discussion



## Atmospheric boundary layer top height in South Africa

K. Korhonen et al.

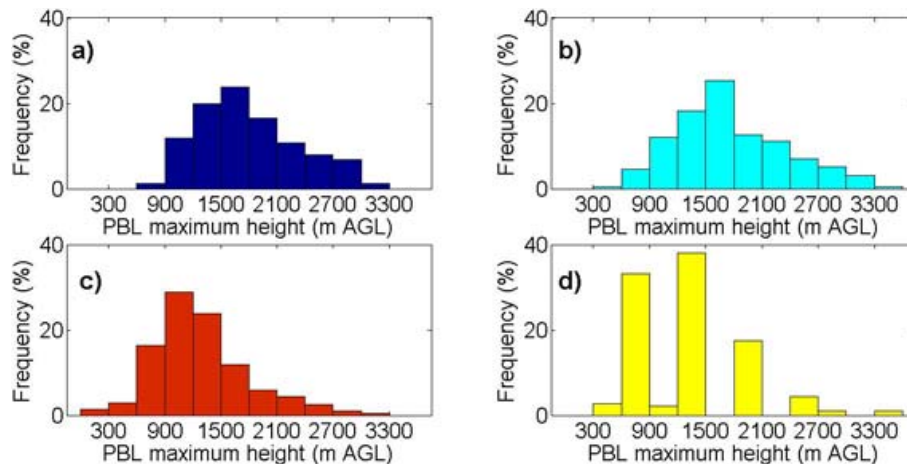


**Fig. 6.** Histograms for measured and modelled PBL top daily maximum heights during 2010, (a) Polly<sup>XT</sup>, (b) ECMWF, (c) TAPM and (d) SAWS.

[Title Page](#)[Abstract](#)[Introduction](#)[Conclusions](#)[References](#)[Tables](#)[Figures](#)[◀](#)[▶](#)[◀](#)[▶](#)[Back](#)[Close](#)[Full Screen / Esc](#)[Printer-friendly Version](#)[Interactive Discussion](#)

Atmospheric  
boundary layer top  
height in South Africa

K. Korhonen et al.

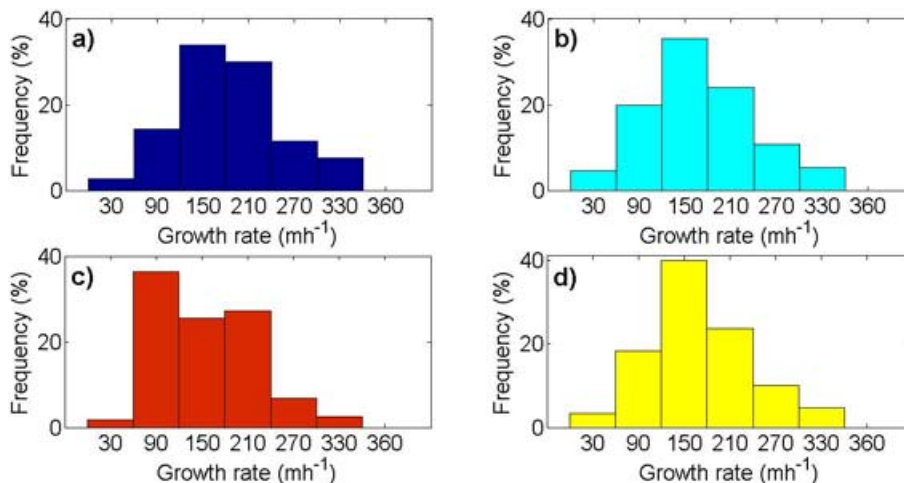


**Fig. 7.** PBL growth rates during the comparison period, **(a)** Polly<sup>XT</sup>, **(b)** ECMWF, **(c)** TAPM and **(d)** SAWS.

[Title Page](#)[Abstract](#)[Introduction](#)[Conclusions](#)[References](#)[Tables](#)[Figures](#)[◀](#)[▶](#)[◀](#)[▶](#)[Back](#)[Close](#)[Full Screen / Esc](#)[Printer-friendly Version](#)[Interactive Discussion](#)

## Atmospheric boundary layer top height in South Africa

K. Korhonen et al.

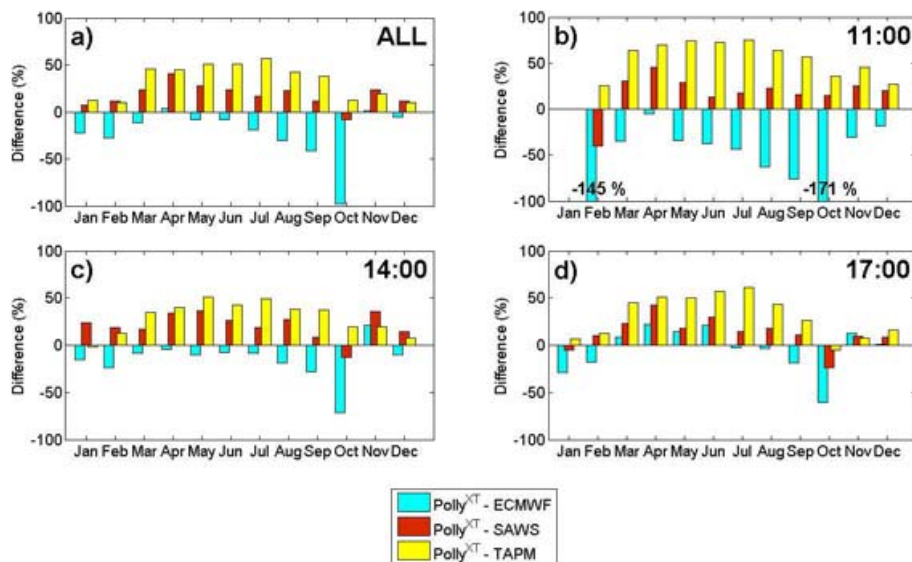


**Fig. 8.** Monthly mean differences in PBL height from the lidar and each model, **(a)** all values between 11:00–17:00, **(b)** 11:00, **(c)** 14:00 and **(d)** 17:00 LT.

Atmospheric  
boundary layer top  
height in South Africa

K. Korhonen et al.

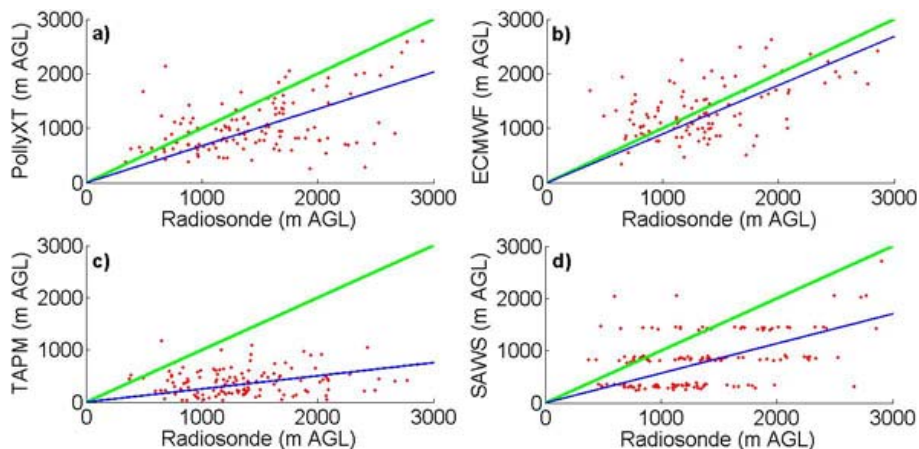


**Fig. 9.** Scatterplots for comparing Polly<sup>XT</sup> (a), the ECMWF (b), TAPM (c) and the SAWS model (d) to radiosonde observations in the comparison period. Blue and green lines mark linear fit to the data and 1 : 1 correlation, respectively.

[Title Page](#)[Abstract](#)[Introduction](#)[Conclusions](#)[References](#)[Tables](#)[Figures](#)[◀](#)[▶](#)[◀](#)[▶](#)[Back](#)[Close](#)[Full Screen / Esc](#)[Printer-friendly Version](#)[Interactive Discussion](#)

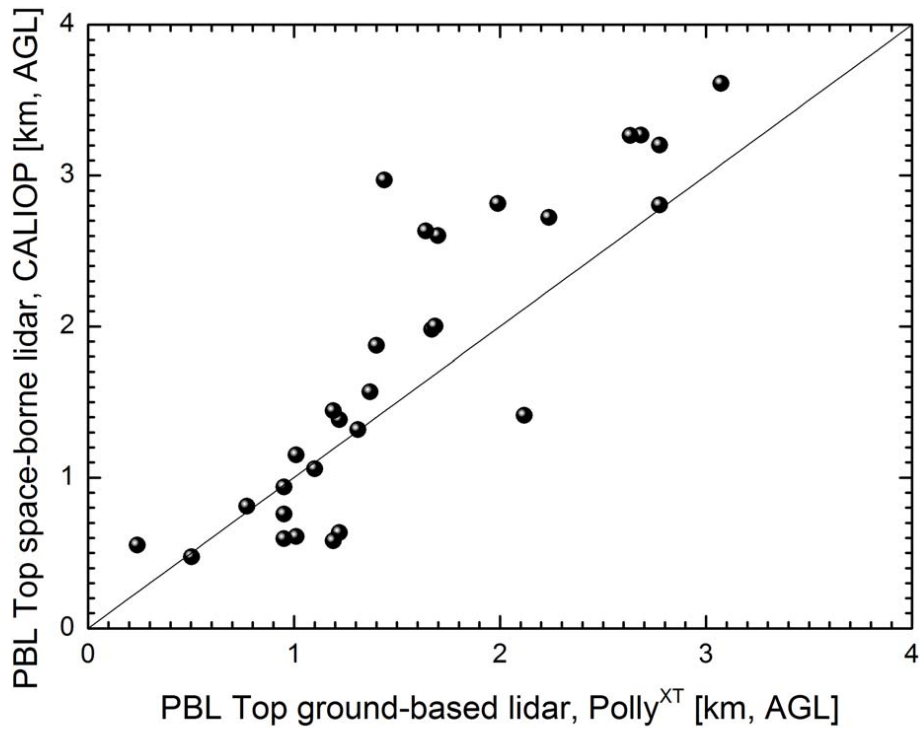


**Fig. 10.** PBL top comparison of 29 common PBL top height observation cases for Polly<sup>XT</sup> and CALIOP data.

**Atmospheric  
boundary layer top  
height in South Africa**

K. Korhonen et al.

Title Page

Abstract

Introduction

Conclusions

References

Tables

Figures

◀

▶

◀

▶

Back

Close

Full Screen / Esc

Printer-friendly Version

Interactive Discussion

